



Title	Stress and Deformation Analysis of REBCO Pancake Coils With Individual Turn Movement
Author(s)	Kodaka, Kazuma; Noguchi, So
Citation	IEEE transactions on applied superconductivity, 33(5), 4600305 <a href="https://doi.org/10.1109/TASC.2023.3237122">https://doi.org/10.1109/TASC.2023.3237122</a>
Issue Date	2023-08
Doc URL	<a href="http://hdl.handle.net/2115/88949">http://hdl.handle.net/2115/88949</a>
Rights	© 2023 IEEE. Personal use of this material is permitted. Permission from IEEE must be obtained for all other uses, in any current or future media, including reprinting/republishing this material for advertising or promotional purposes, creating new collective works, for resale or redistribution to servers or lists, or reuse of any copyrighted component of this work in other works.
Type	article (author version)
File Information	ASC2022-2LPo1B-08_FINAL_VERSION_source.pdf



[Instructions for use](#)

# Stress and Deformation Analysis of REBCO Pancake Coils with Individual Turn Movement

Kazuma Kodaka and So Noguchi

**Abstract**—In recent years, rare-earth barium copper oxide (REBCO) pancake coils have shown excellent performances in high magnetic field applications. The no-insulation (NI) winding technique enables to enhance the thermal stability and current density of REBCO pancake coils. Still, further developments of REBCO coils are expected; e.g., the mechanical deteriorations of REBCO tapes caused by electromagnetic forces have been reported. The screening currents are considered as one of the causes to damage the REBCO tapes because of a nonuniform current distribution. Meanwhile, the electromagnetic forces on non-impregnant NI REBCO coils, whose windings can be deformed separately with turns and moved easily, are complicated, and the detailed mechanism has not yet been clarified. Commonly, the circumferential movement/deformation of the winding is considered as a rigid body. In this study, we investigate the stresses and displacements due to the electromagnetic forces on NI REBCO pancake coils in high magnetic field using a current simulation and a 2D elastic finite element analysis in the radial and circumferential directions; i.e., each turn can individually move in the radial and circumferential directions considering the spiral winding structure. The simulation results show the circumferential movement/deformation of windings and the nonuniform hoop stress due to the electromagnetic force.

**Index Terms**— Deformation analysis, high magnetic field, no-insulation winding technique, REBCO coil.

## I. INTRODUCTION

IN recent years, rare-earth barium copper oxide (REBCO) pancake coils have made great progresses in high field applications. In particular, the no-insulation (NI) winding technique improves the thermal stability and current density of REBCO pancake coils by removing any insulation layer between turns [1]–[3]. Further developments of REBCO pancake coils for high field applications such as nuclear magnet resonance (NMR), magnetic resonance imaging (MRI), particle accelerators, and fusion devices are expected [4]–[11].

Meanwhile, mechanical damages and critical current ( $I_c$ ) deteriorations of REBCO tapes have been reported [12]. In high magnetic field, an excessive force applied to a REBCO tape

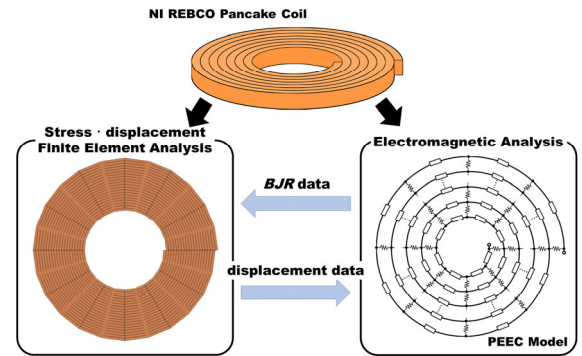


Fig. 1. NI REBCO pancake coil simulation coupling electromagnetic and stress/displacement analysis.

would cause degradations or distortions, which prevent the REBCO coil from a stable magnetic field generation. The screening current has been considered as one of the causes of this problem [13]–[16]. Due to the magnetic field generated perpendicular to the wide REBCO tape surface, the screening current induced on the longitudinal edges of REBCO tape leads to nonuniform current distribution on the cross section of the winding. Thus, strong electromagnetic forces generate large distortions to coil windings. So far, the detailed mechanism of such damages has not been clarified. Furthermore, unlike impregnated coils, the deformation of NI REBCO coil is much complicated because each turn can independently, separately and easily move in both the circumferential and radial directions. Although a REBCO pancake coil consisting of one continuous tape may move circumferentially as well as radially, previously reported simulations have considered only the radial deformation of windings as a rigid body [17].

To investigate the mechanism of damages in the REBCO coils, deformations, including turn-separate movement keeping the spiral winding structure, should be evaluated. In this study, we investigate the stresses and deformations due to the electromagnetic forces on the REBCO pancake coils in high magnetic field by numerical simulation considering individual-turn movement.

## II. SIMULATION METHOD

In the developed in-house code, electromagnetic and stress/displacement simulations of NI REBCO pancake coils are coupled as shown in Fig. 1. The current behavior is computed with the partial element equivalent circuit (PEEC)

Manuscript receipt and acceptance dates will be inserted here. Acknowledgment of support is placed in this paragraph as well. Consult the IEEE Editorial Style Manual for examples. This work was supported by the JSPS KAKENHI under Grant 20H02125. (Corresponding author: So Noguchi.)

K. Kodaka and S. Noguchi are with the Graduate School of Information Science and Technology, Hokkaido University, Sapporo 060-0814, Japan (e-mail: kodaka@em.ist.hokudai.ac.jp; noguchi@ssi.ist.hokudai.ac.jp).

Color versions of one or more of the figures in this paper are available online at <http://ieeexplore.ieee.org>.

Digital Object Identifier will be inserted here upon acceptance.

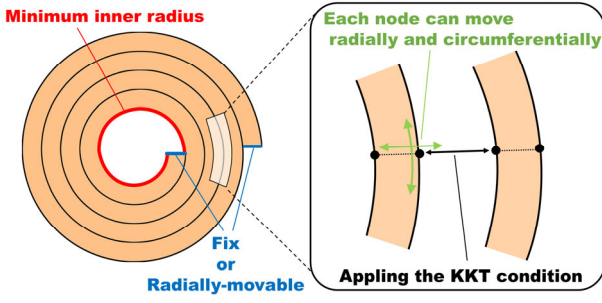


Fig. 2. The simulation model of FEM and boundary conditions considering turn separation.

method [3], [18]. The stress and displacement are computed by two-dimensional (2D) finite element method (FEM) with the  $BJR$  stress as an input.

In the PEEC method, an NI REBCO coil is subdivided into the circumferential and radial directions to obtain the detailed current distribution. The PEEC model has been shown to be effective in many previous studies [19], [20]. The REBCO layer resistance in the PEEC model is approximated with the  $n$ -index model based on  $I$ - $V$  characteristics [21].

The stress/displacement simulation is performed with 2D FEM on the  $r\theta$  plane. Fig. 2 shows the simulation model of FEM considering turn separation. The following equilibrium equations are adopted as governing equations to each finite element:

$$\frac{\partial \sigma_r}{\partial r} + \frac{1}{r} \frac{\partial \sigma_{r\theta}}{\partial \theta} + \frac{\sigma_r - \sigma_\theta}{r} + J_\theta B_z = 0 \quad (1)$$

$$\frac{\partial \sigma_{r\theta}}{\partial r} + \frac{1}{r} \frac{\partial \sigma_\theta}{\partial \theta} + \frac{\sigma_{r\theta} + \sigma_{\theta r}}{r} - J_r B_z = 0 \quad (2)$$

where  $\sigma_r$ ,  $\sigma_\theta$ ,  $\sigma_{r\theta}$ ,  $J_r$ ,  $J_\theta$ , and  $B_z$  are the radial stress, the circumferential stress, the shear stress around  $z$ -axis, the radial current density, the circumferential current density, and the axial magnetic flux density, respectively. (1) and (2) indicate the radial and circumferential equilibriums, separately. Friction between turns is not considered in this study.  $J_r$ ,  $J_\theta$ , and  $B_z$  of each element are obtained from the electromagnetic simulation of PEEC model.

In the simulation, to consider turn separation, the following Karush-Kuhn-Tucker (KKT) condition [22] is employed to avoid adjacent tapes from overlapping each other.

$$\begin{cases} \frac{\partial W}{\partial \mathbf{u}} + \mu \frac{\partial G}{\partial \mathbf{u}} = 0 \\ \mu \geq 0 \\ \mu G(\mathbf{u}) = 0 \end{cases} \quad (3)$$

where  $W$  and  $G$  are the objective function which is derived from the FEM in this paper and the constraint condition function which is the distance between adjacent nodes.  $\mu$  indicates the penalty parameter corresponding to the restraining force. These KKT equations with FEM are solved with the Newton-Raphson method as a nonlinear problem.

In designing REBCO pancake coils, two fixed terminals with current leads are indispensable. However, in this simulation where the winding deforms turn-independently in the ra-

TABLE I  
SPECIFICATIONS OF REBCO TAPES AND PANCAKE COILS

Parameters	Values
REBCO Tape	
Tape width [mm]	4.0
REBCO tape thickness [mm]	0.1
Copper matrix thickness [ $\mu\text{m}$ ]	20.0
REBCO layer thickness [ $\mu\text{m}$ ]	2.0
$n$ -index	30
$I_c$ @ 77 K, self-field [A]	120.0
Poisson's ratio	0.32
Young's module [GPa]	200
Single Pancake Coil	
Coil inner diameter [mm]	60.0
Azimuthal divisions	12
Contact resistivity [ $\mu\Omega \cdot \text{cm}^2$ ]	70.0

TABLE II  
SIMULATION CONDITIONS

Parameters	Values
Number of turns	20, 40, 60
External magnetic field [T]	0, 40
Operating temperature [K]	20.0
Operating current [A]	300
Terminal conditions	fixed or radially-movable

dial and circumferential directions, the fixed terminals may affect the mechanical behaviors of REBCO pancake coils. Hence, we investigated two cases: (1) fixed terminals and (2) radially-movable terminals as a boundary condition. It is assumed that the initial position of the innermost turn is set to the minimum radius supposing a bobbin.

### III. SIMULATION RESULTS

Table I lists the specifications of REBCO tapes and REBCO pancake coils. In this paper, the REBCO tapes are assumed as a homogeneous structure, and the physical properties, Young's module and Poisson's ratio, of Hastelloy are adopted for the stress/strain simulation. We have performed a few simulations with different conditions listed in Table II. It is also assumed that an external magnetic field in the axial direction is applied uniformly to the REBCO pancake coil by an outsert magnet. We will discuss about the effect of the deformation in the circumferential direction and the differences in the cases of fixed terminals and radially-movable terminals from the obtained simulation results below.

#### A. Mechanical behaviors of NI REBCO pancake coils with turn-separate deformation

Figs. 3 and 4 respectively show the distributions of the displacement in the circumferential direction, the hoop stress, and the  $BJR$  stress in the cases of 0-T and 40-T external magnetic fields for the 40-turn REBCO pancake coil with fixed terminals.

From the simulation result of no external field, the deformation in the circumferential direction can hardly be seen. The hoop stress agrees with the  $BJR$  stress well.

Meanwhile, the circumferential deformation of NI REBCO pancake coils due to the electromagnetic force can be observed in the case of high external field (40 T). The coil wind-

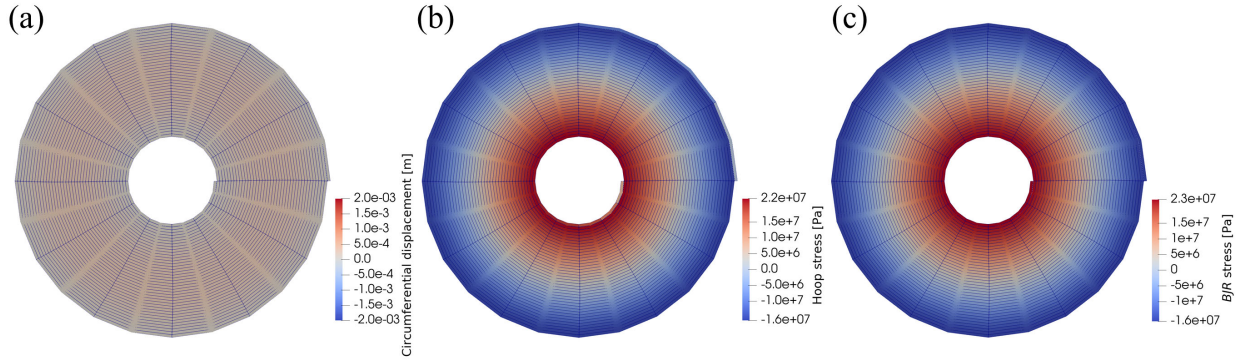


Fig. 3. Distributions of (a) circumferential displacement, (b) hoop stress, and (c) *BJR* stress without external magnetic field (not to scale).

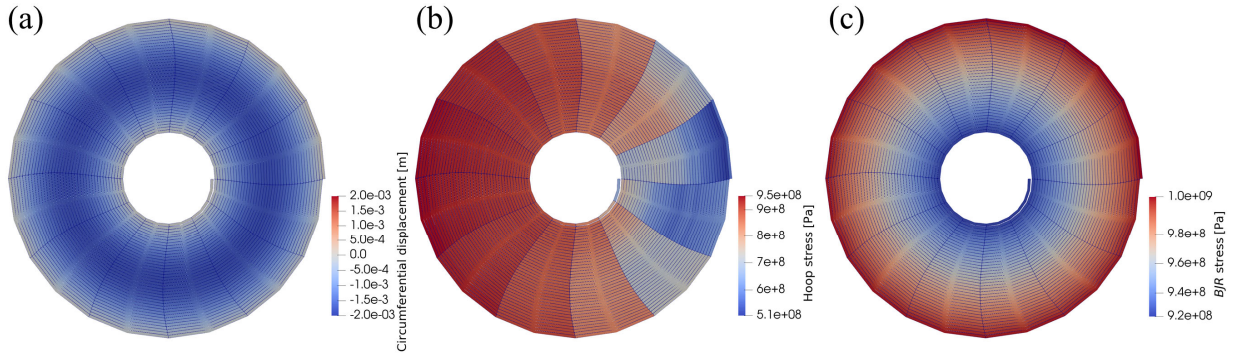


Fig. 4. Distributions of (a) circumferential displacement, (b) hoop stress, and (c) *BJR* stress with 40-T external magnetic field (not to scale).

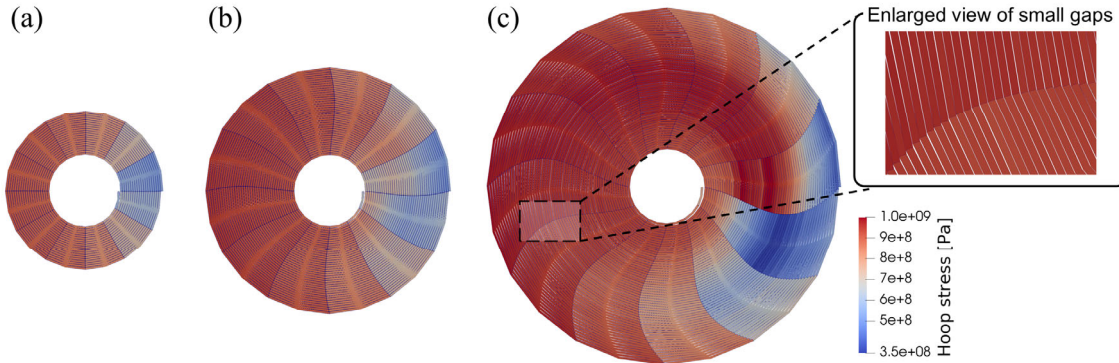


Fig. 5. Comparison of circumferential stress distributions for different number of turns [(a) 20, (b) 40, and (c) 60 turns] with 40-T external magnetic field (not to scale).

ing tends to extend in the radial direction because of the strong electromagnetic force, whereas it is also deformed in the circumferential direction by turn-separate movement together with relaxation of hoop stress. The hoop stress pattern in 40 T is completely different from that in 0 T. Consequently, it can be considered that the circumferentially rotational movement reduces the hoop stress by balancing the electromagnetic forces on the whole coil winding. The middle turns of the coil greatly moves in the circumferential direction. There is a large space between the innermost turn and the next turn around the inner fixed terminal.

Fig. 5 shows the comparison of the circumferential stresses for different number of turns (20, 40, and 60 turns). As the REBCO pancake coil increases in the number of turns, the circumferential deformation also increases because a longer winding makes more allowances for rotational movement. De-

spite the high hoop stress in the 60-turn case, the stress around the outer terminal is smaller than that in the 20- and 40-turn coils. Furthermore, particularly in the 60-turn coil, a few slight gaps can be seen between turns in the opposite of the terminals, as shown in the inset of Fig. 5. These gaps are considered the effects of fixed terminals. In the pancake coil where the terminals are fixed and each turn moves separately, the circumferential movement of windings causes some deflection. The large deflection results in more circumferential deformation in the case of the greater number of turns. The deflection is concentrated on the opposite of the terminals, where windings can move easily in the radial direction. Accordingly, the hoop stress distribution is also nonuniform.

From these results, the circumferential deformation enables to suppress the hoop stresses, whereas it generates small gaps between turns. These gaps possibly deteriorate the turn-to-turn



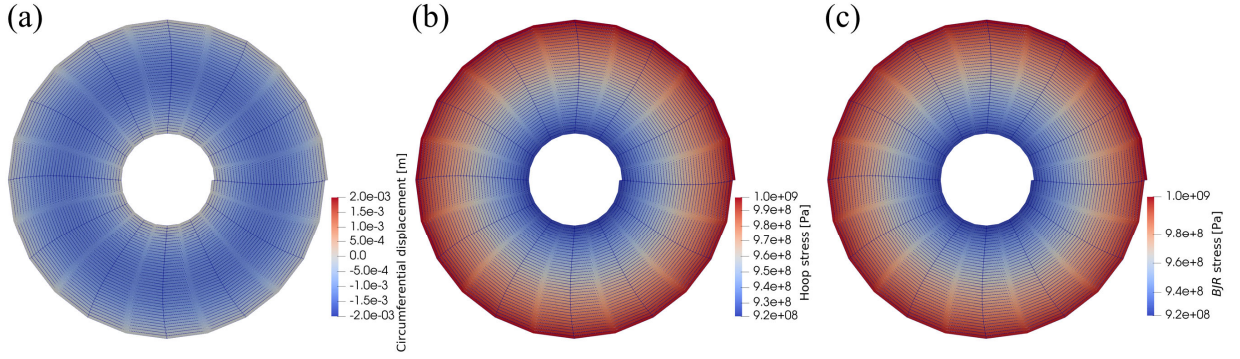


Fig. 6. Distributions of (a) circumferential displacement, (b) hoop stress, and (c)  $BJR$  stress with 40-T external magnetic field and radially-movable terminals (not to scale).

contact condition so that the contact resistance increases and the bypassing current in radial direction is disturbed. Eventually the thermal stability of NI REBCO pancake coils may be degraded. Further investigations on the thermal stability are needed in the near future.

#### B. Comparison with fixed and radially-movable terminals

Fig. 6 shows the distributions of the displacement in the circumferential direction, the hoop stress, and the  $BJR$  stress in the cases of 40-T external magnetic fields for the 40-turn REBCO pancake coil with radially-movable terminals. Although the nonuniform hoop stress is generated in the fixed terminals case as shown in Figs. 4 and 5, the circumferentially uniform distribution of hoop stress in the radially-movable case can be seen from the results. The hoop stress is almost identical to the  $BJR$  stress. Also, no gaps between turns were observed in radially-movable terminals.

Fig. 7 shows the plots of the hoop stress of the analytical solution [17], the obtained simulation results of the maximum stress in each turn with fixed terminals and radially-movable ones, where  $\rho$  is the radial position normalized by the inner radius. In both cases of fixed and radially-movable terminals considering turn-separation, the normalized hoop stress is larger on the outer turns consistent with the  $BJR$  stress. The hoop stress with radially-movable terminals is greater than that with fixed terminals in each turn due to the less circumferential deformation.

The electromagnetic forces on the REBCO coil are balanced over the winding by radially-movable terminals. Thus, the simulation results with radially-movable terminals are expected to be close to the conventional stress which is the analytical solution as a rigid body. The result considering turn-separate movement is significantly different from the analytical result. According to the distribution of  $BJR$  stress, the simulation result seems more appropriate because the outer turns of the REBCO coil have the larger electromagnetic force. Furthermore, the maximum hoop stress is suppressed more than that in the analytical solution due to slight deformation in the circumferential direction even in the case of radially-movable terminals.

From these results, we confirmed the behavior of the NI RECO pancake coil with radially-movable terminals and the

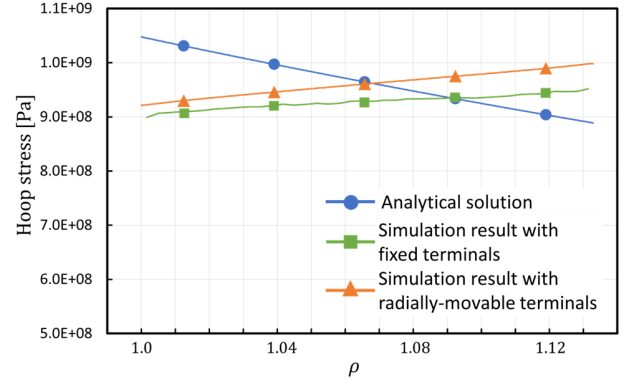


Fig. 7. Plots of the hoop stress of the analytical solution, the simulation results of the maximum stress in each turn with fixed terminals and radially-movable terminals.

validity of the developed simulation. The hoop stress of the REBCO pancake coil can be circumferentially uniformed by radially-movable terminals.

#### IV. CONCLUSION

We have developed an electromagnetic and stress/displacement simulation method for NI REBCO pancake coils considering individually turn-separate movement using the PEEC method and the 2D elastic FEM. Also, the difference of terminal conditions has been investigated. The findings from the simulation results about the circumferential deformation of NI REBCO pancake coils in high magnetic field and the effect of fixed terminals are summarized as follows:

1. The winding of NI REBCO pancake coils in high magnetic fields is deformed in the circumferential direction to suppress the hoop stresses produced by the radial electromagnetic force. This effect is enhanced as the number of turns increases.
2. Large circumferential deformations produce some gaps inside the coil. These gaps may degrade the thermal stability of NI REBCO pancake coils by deterioration of the contact conditions between turns.
3. Fixed terminals with current leads cause the circumferentially nonuniform distribution of hoop stresses.

The effects of metal reinforcement like over-band or YOROI structure [23] should be investigated in the near future.

## REFERENCES

- [1] S. Hahn, D. K. Park, J. Bascuñán, and Y. Iwasa, "HTS pancake coils without turn-to-turn insulation," *IEEE Trans. Appl. Supercond.*, vol. 21, no. 3, pp. 1592–1595, Jun. 2011.
- [2] S. Choi, *et al.*, "A study on the no insulation winding method of the HTS coil," *IEEE Trans. Appl. Supercond.*, vol. 22, no. 3, Jun. 2012, Art. no. 4904004.
- [3] T. Wang, *et al.*, "Analyses of transient behaviors of no-insulation REBCO pancake coils during sudden discharging and overcurrent," *IEEE Trans. Appl. Supercond.*, vol. 25, no. 3, Jun. 2015, Art. no. 4603409.
- [4] Y. Iwasa, *et al.*, "A high-resolution 1.3-GHz/54-mm LTS/HTS NMR magnet," *IEEE Trans. Appl. Supercond.*, vol. 25, no. 3, Jun. 2015, Art. no. 4301205.
- [5] H. Miyazaki, *et al.*, "Design of a conduction-cooled 9.4 T REBCO magnet for whole-body MRI systems," *Supercond. Sci. Technol.*, vol. 29, no. 10, Aug. 2016, Art. no. 104001.
- [6] S. Yokoyama, *et al.*, "Research and development of the high stable magnetic field ReBCO coil system fundamental technology for MRI," *IEEE Trans. Appl. Supercond.*, vol. 27, no. 4, Jun. 2017, Art. no. 4400604.
- [7] T. F. Budinger, *et al.*, "Toward 20 T magnetic resonance for human brain studies: Opportunities for discovery and neuroscience rationale," *Magn. Reson. Mater. Phys.*, vol. 29, no. 3, pp. 617–639, Jun. 2016.
- [8] H. Ueda, *et al.*, "Conceptual design of next generation HTS cyclotron," *IEEE Trans. Appl. Supercond.*, vol. 23, no. 3, Jun. 2013, Art. no. 4100205.
- [9] J. Nugteren, *et al.*, "Toward REBCO 20 T+ dipoles for accelerators," *IEEE Trans. Appl. Supercond.*, vol. 28, no. 4, Jun. 2018, Art. no. 4008509.
- [10] P. Bruzzone, *et al.*, "High temperature superconductors for fusion magnets," *Nuclear Fusion*, vol. 58, no. 10, Aug. 2018, Art. No. 103001.
- [11] A. Sagara, *et al.*, "Two conceptual designs of helical fusion reactor FFHR-d1A based on ITER technologies and challenging ideas," *Nuclear Fusion*, vol. 57, no. 8, Jul. 2017, Art. No. 086046.
- [12] S. Hahn, *et al.*, "45.5-tesla direct-current magnetic field generated with a high-temperature superconducting magnet," *Nature*, vol. 570, no. 7762, pp. 496–499, Jun. 2019.
- [13] J. Xia, *et al.*, "Stress and strain analysis of a REBCO high field coil based on the distribution of shielding current," *Supercond. Sci. Technol.*, vol. 32, no. 9, Jul. 2019 Art. no. 095005.
- [14] Y. Li, *et al.*, "Magnetization and screening current in an 800 MHz (18.8 T) REBCO nuclear magnetic resonance insert magnet: experimental results and numerical analysis," *Supercond. Sci. Technol.*, vol. 32, no. 23, Aug. 2019 Art. no. 105007.
- [15] Y. Yan, C. Xin, M. Guan, H. Liu, Y. Tan, and T. Qu, "Screening current effect on the stress and strain distribution in REBCO high-field magnets: Experimental verification and numerical analysis," *Supercond. Sci. Technol.*, vol. 33, no. 5, Mar 2020, Art. no. 05LT02.
- [16] H. Ueda, K. Naito, and S.B. Kim, "Deformation analysis of no-insulation REBCO coils considering turn-to-turn contact configuration," *IEEE Trans. Appl. Supercond.*, vol. 32, no. 6, Jun. 2022, Art. no. 4604205.
- [17] Y. Iwasa, "Case Studies in Superconducting Magnets: *Design and Operational Issues*," Springer, 2009, p.98-104.
- [18] R. Miyao, H. Igarashi, A. Ishiyama, and S. Noguchi, "Thermal and electromagnetic simulation of multistacked no-insulation REBCO pancake coils on normal-state transition by PEEC method," *IEEE Trans. Appl. Supercond.*, vol. 28, no. 3, Apr. 2018, Art. no. 4601405.
- [19] W. D. Markiewicz, J. J. Jaroszynski, D. V. Abaimov, R. E. Joyner, and A. Khan, "Quench analysis of pancake wound REBCO coils with low resistance between turns," *Supercond. Sci. Technol.*, vol. 29, Dec. 2015, Art. no. 025001.
- [20] Y. Wang, W. K. Chan, and J. Schwartz, "Self-protection mechanism in no-insulation (RE)Ba<sub>2</sub>Cu<sub>3</sub>O<sub>x</sub> high temperature superconductor pancake coils," *Supercond. Sci. Technol.*, vol. 29, Mar. 2016, Art. no. 045007.
- [21] V. Selvamanickam, *et al.*, "The low-temperature, high-magnetic-field critical current characteristics of Zr-added (Gd, Y) Ba<sub>2</sub>Cu<sub>3</sub>O<sub>x</sub> superconducting tapes," *Supercond. Sci. Technol.*, vol. 25, Oct. 2012, Art. no. 125013.
- [22] H. W. Kuhn and A. W. Tucker, "Nonlinear programming," *Proceeding of the Second Berkeley Symposium on Mathematical Statics and Probability*, University of California Press, 1951, pp. 481-492.
- [23] S. Nagaya, *et al.*, "Development of high strength pancake coil with stress controlling structure by REBCO coated conductor," *IEEE Trans. Appl. Supercond.*, vol. 23, no. 3, Jun. 2013, Art. no. 4601204.